Available online at www.sciencedirect.com
SCIENCE DIRECT
Journal of Power Sources 154 (2006) 404–411
JOURNAL OF POWER SOURCES
www.elsevier.com/locate/jpowsour

Low temperature operation and influence parameters on the cold start ability of portable PEMFCs

M. Oszcipok *, M. Zedda, D. Riemann, D. Geckeler

Fraunhofer Institute for Solar Energy Systems, Heidenhofstr. 2, Germany

Available online 21 November 2005

Abstract

The start up behaviour of PEM fuel cells below 0 °C is one of the most challenging tasks to be solved before commercialisation. The automotive industry started to develop solutions to reduce the start up time of fuel cell systems in the middle of the nineties. The strategies varied from catalytic combustion of hydrogen on the electrode catalyst to fuel starvation or external stack heating via cooling loops to increase the stack temperature.

Beside the automotive sector the cold start ability is as well important for portable PEMFC applications for outdoor use. But here the cold start issue is even more complicated, as the fuel cell system should be operated as passive as possible.

Below 0 °C freezing of water inside the PEMFC could form ice layers in the electrode and in the gas diffusion layer. Therefore the cell reaction is limited or even inhibited. Product water during the start up builds additional barriers and leads to a strong decay of the output power at isothermal operating conditions.

In order to find out which operational and hardware parameters affect this decay, potentiostatic experiments on single cells were performed at isothermal conditions. These experiments comprise investigations of the influence of membrane thickness and different GDL types as well as the effect of gas flow rates and humidification levels of the membrane. As pre stage to physical based models, empirical based prediction models are used to gain a better understanding of the main influence parameters during cold start. The results are analysed using the statistical software Cornerstone 4.0.

The experience of single cell investigations are compared to start up behaviour of portable fuel cell stacks which are operated in a climate chamber at different ambient temperatures below 0 °C. Additional flow sharing problems in the fuel cell stack could be seen during cold start up experiments.

Keywords: PEMFC; Cold start; Portable fuel cells; Statistical analysis; Degradation

1. Introduction

Fuel cells are known as one of the most promising energy conversion systems for the future. Their principle of direct conversion of chemical energy into electrical energy and heat let them fit to various applications. Especially the automotive industry pushed the PEMFC development in the recent years strongly. Beside very high dynamic demands in cars fuel cell systems must also be able to start at temperatures below 0 °C.

Operational demands in other fuel cell applications are normally much lower. For portable applications with a fuel cell system power below 100 W a lot of promising systems were presented which show good performance data at ambient conditions [1–4].

But especially for the advanced hydrogen/air PEMFC technology new challenges come up. The ability to deliver power to outdoor applications like independent power sources for outdoor environment or traffic gauging stations demands cold start ability of a fuel cell system.

Compared to the automotive fuel cell systems portable PEMFC systems should be more simple. For cold start no peripheral system components should be used with respect to the overall system efficiency. The aim of our investigations was to find out the main influencing parameters on the fuel cell cold start ability covering operational parameters and hardware parameters in single fuel cells as well as in portable fuel cell stacks.

* Corresponding author. Tel.: +49 761 4588 5432; fax: +49 761 4588 9432.
E-mail address: michael.oszcipok@ise.fraunhofer.de (M. Oszcipok).

0378-7753/$ – see front matter © 2005 Elsevier B.V. All rights reserved.
doi:10.1016/j.jpowsour.2005.10.035

2. Experimental set-up

2.1. Single cell test bench

A test bench was set-up which enables single fuel cell operation at nearly isothermal conditions. The temperature (between −16 and 70 °C) can be controlled by a cryostat bath (Lauda) which is connected to the fuel cell cooling plates. The gas humidity is adjustable up to 100% using conventional bubble humidifiers. The gas inlet and outlet pressures, dew points, and temperatures are monitored as well as the cell temperature of the anode and cathode graphite flowfield plate. The whole test bench is controlled automatically by LabView©. All signals are recorded by a data logger (Agilent). For gas regulation digital mass flow controllers (Bronkhorst) are used. The electronic load (Zentro EL) has an operating range up to 50 A.

The single test cell has an active area of 46 cm^2. The flowfield has a double serpentine structure with a channel width of 1.2 mm, depth 0.8 mm and a ligament width of 1.2 mm. The fuel cell assembly, comprising the catalyst coated membrane, gas diffusion layer (GDL), graphite compound flowfield plates, titanium end plates, and plastic cooling plates are placed in an isolation housing made of Styrodur© C to minimize the impact of heat exchange with the ambience.

2.2. Climatic chamber test bench

For realistic fuel cell system testing a test bench with a climatic chamber (Vötsch VC 4034) was set-up. Fuel cell systems and fuel stack operational behaviour can be investigated in a range between −40 and 100 °C and 10% and 98% r.h. All main components are controlled by LabView© and all signals are monitored via data logger and PCI measuring PC card. Gases can be supplied humidified or dry to the fuel cell. The electronic load (Zentro EL) can operate up to 125 A.

The fuel cell stacks consist of six cells with an active area of 30 cm^2 of each cell. Bipolar plates were made of graphite compound with milled double serpentine flowfields. The current collectors are made of copper and the endplates of aluminium.

The fuel cell stack was placed in a plastic housing, to prevent convective cooling by the climate chamber fan. The air is supplied by a pump (Nitto) which delivers cold air from the interior of the climate chamber. Dry hydrogen is supplied by the test bench and the gas temperature is reduced by cooling coils inside the climate chamber interior.

3. Experimental and statistical analysis

3.1. Single cell cold start experiments

Before freezing the fuel cell a reference performance measurement at 0.45 V with dry hydrogen (stoichiometry 1.5) and dry air (stoichiometry 3.0) at 30 °C was recorded. This reference power density is called p_{450}. Each point was measured at least 20 min, gas flows were adjusted automatically to the actual current.

Table 1
Varied operating parameters for start up experiments at −10 °C

Operating parameter	Values
Applied voltage for cold start up, V (mV)	200/400/600
Air flow rate, u_{air} (ml min^{-1})	147–1000
Hydrogen flow rate, u_{H_2} (ml min^{-1})	20–158
Cell impedance after nitrogen purging, $Z_{purging}$ (mΩ)	70–1500
Cell impedance after applying gases directly before cold start, Z_{start} (mΩ)	7–50
Power density at 450 mV, 30 °C, dry gases, stoichiometry 1.5/3.0, p_{450} (mW cm^{-2})	210–350

After this reference operation the gases were switched to dry nitrogen (N_2) and both sides of the fuel cell were purged with 1.0 l min^{-1} at 30 °C. The purging process continued until the cell impedance at 1000 Hz increases from 2.5 to 4.5 mΩ at normal operation conditions to values larger than 500 mΩ. Then N_2 flow is switched off and the cell is cooled down.

After drying and freezing of the cell, the start up experiments were carried out potentiostatically. Gas flow rates were kept constant as well as the cell temperature. When the graphite plates reach the required temperature, dry hydrogen and dry air is switched on. After open circuit voltage has arisen potentiostatic load is applied. The cumulated charge transfer density $S_{q,cum}(t)$ serves for evaluation of the cold start experiments and is calculated by (1)

$$S_{q,cum}(t) = \int_0^t i \, dt \tag{1}$$

$S_{q,cum}(t)$ is chosen because it is very useful to compare different cold start experiments with each other. The higher $S_{q,cum}(t)$ the better is the cold start behaviour. On the other hand $S_{q,cum}(t)$ directly correlates with the amount of product water $m_{H_2O,prod}$ given by Eq. (2)

$$m_{H_2O,prod} = \frac{S_{q,cum}(t)}{2F} M_{H_2O} \tag{2}$$

In (2) $m_{H_2O,prod}$ is the area specific product water weight in g cm^{-2}, $S_{q,cum}(t)$ the cumulated charge transfer density in C cm^{-2}, F the Faraday constant 96,485 C mol^{-1} and M_{H_2O} is the molar weight of water in g mol^{-1}.

3.2. Experimental cold start influence parameters

To find out the main influencing operating parameters 15 experiments were carried out at constant temperature of −10 °C. In Table 1 all varied operating parameters are listed and explained.

In a second experimental series the influence of cell components was studied. In Table 2 the varied fuel cell components

Table 2
Varied component parameters for −10 °C start up experiments

Parameter	Values
MEA, membrane thickness	18/25/35
Gas diffusion layer	GDL/MPL/OAC/OCC

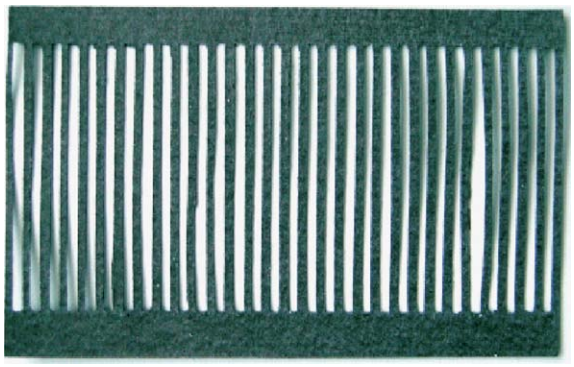

Fig. 1. Open channel gas diffusion layer. The reaction gas can diffuse under the landing of the double serpentine flowfield while the electrode under the channels is directly exposed to the gas stream.

are listed. Catalyst coated membranes are used with a platinum catalyst loading of 0.4 $mg_{Pt}\,cm^{-2}$ on both electrodes. As gas diffusion layer (GDL) carbon cloth was used with a thickness of 190 μm, a porosity of 0.75 and a PTFE content of 10%. Experiments with standard GDL were performed as well as experiments with additional micro porous carbon layers (MPL) on both electrodes.

In further experiments the GDL were cut in a way, that one electrode surface, either the anode (OAC, open anode channels) or the cathode (OCC, open cathode channels) is directly exposed to the gas stream while the other electrode is equipped with a standard GDL. Fig. 1 shows an open channel GDL.

3.3. Data analysis using statistical prediction models

The statistical software Cornerstone® (Brooks Automation) fits a response y, e.g. $S_{q,\mathrm{cum}}(t)$, with a polynomial term consisting of a constant c, the values x_i of the p influence parameters, e.g. applied voltage V, multiplied by constant factors a_i. In (3) a polynomial term is shown, where linear effects are taken into account in the first term, interaction effects between each parameter in the second term and quadratic effects in the third term

$$y = c + \sum_{i=1}^{p} a_i x_i + \sum_{\substack{i,\, j=1 \\ i \neq j}}^{p} a_{ij} x_{ij} + \sum_{i=1}^{p} a_{ii} x_i^2 \tag{3}$$

The fit quality of the regression polynomial is evaluated by the stability index R^2 and the adjusted stability index R^2_{adj}. R^2 is the relation between the statistical spread of the model and the statistical spread of the real measured values. For test series with a low number of experiments R^2_{adj} is better suited, because it accounts additionally for the number experiments and the number of influence parameters. The values of R^2 and R^2_{adj} are between 0 and 1. For serious statements R^2_{adj} should normally be higher than 0.8 [5,6].

3.4. Portable fuel cell stack cold start experiments

To investigate the starting behaviour of fuel cell stacks two test series were performed at −10 and −20 °C. Fuel cell stacks were dried by N_2 purging whereby the stack impedance increased from its normal value of 20 to 100 mΩ and above. The gas flow rates for start up were kept constant as long as possible on 220 ml min^{-1} H_2 and 600 ml min^{-1} air. These flow rates allow a maximum stack current of more than 5 A. Measurable is the deviation of the single cell voltages from the average cell voltage and the time until the fuel cell stack temperature reaches 0 °C.

4. Single fuel cell results and discussion

4.1. Single fuel cell drying

Before the single fuel cell is cooled down below 0 °C the flowfield must be free of water droplets. Therefore drying of the fuel cell was carried out until the cell impedance reaches more than 500 mΩ. If the purging process is stopped at lower impedance values ice blockages in the gas channels were observed. This occurred in the anode and also the cathode flowfield, detected by increasing inlet pressures when hydrogen and air are applied. Because of the fast water uptake of polymer electrolyte membranes [7] rest humidity from the electrodes and the GDL diffuses back into the membrane when the drying process is stopped and impedance could drop down.

4.2. Single fuel cell operation at −10 °C and parameterisation of results

After the fuel cell is dried out, cooled down to −10 °C and V_{OC} has arisen, potentiostatic load is applied. The resulting current is decreasing over time always with the same principle behaviour. Fig. 4 shows a typical current decay curve over time. The fuel cell is reacting with a fast increase of current which reaches within the first 2 min its maximum and then decays. Also illustrated in Fig. 4 is the cumulated charge transfer density $S_{q,\mathrm{cum}}(t)$. To predict the maximum cumulated charge transfer density $S_{q,\max}$ a mathematical fitting function was found which parameterises $S_{q,\mathrm{cum}}(t)$. This exponential function is calculated by (4)

$$S_{q,\mathrm{fit}}(t) = S_{q,\max}(1 - \mathrm{e}^{-(t/t_{63})^c}) \tag{4}$$

t_{63} is the time when $S_{q,\mathrm{fit}}(t)$ reaches 63% of $S_{q,\max}$ and in combination with the variable c it describes the slope of the curve. This mathematical fitting curve is also shown in Fig. 2. The quality of a cold start experiment is evaluated by $S_{q,\max}$ as response parameter in the statistical regression.

Because the pressure drop of hydrogen and air over the flowfield remains stable, we assume that most of the product water is not transported into the channels, but freezes in the porous structure of the GDL and the electrode. As result the reaction is inhibited.

To analyse the initial starting behaviour the current decay is referred to the cumulated charge transfer density $S_{q,\mathrm{cum}}(t)$. Fig. 3 illustrates current density i versus $S_{q,\mathrm{cum}}(t)$ for the same experiment as shown in Fig. 2. For statistical evaluation it is necessary to parameterise these current density curves. A simple

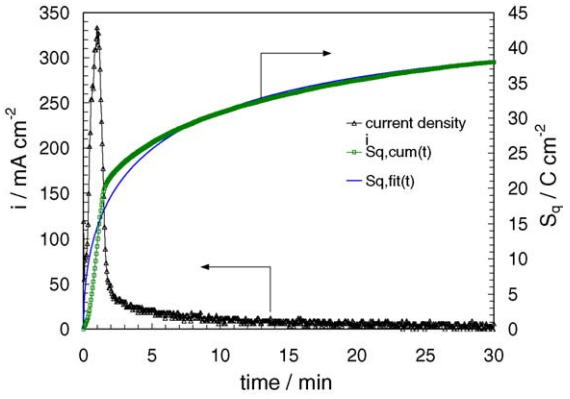

Fig. 2. Decay of current density and cumulated charge transfer over time at a cell voltage of 200 mV, cell temperature: −10 °C, gas flows: 600 ml_{air} min^{-1}, 120 ml_{H_2} min^{-1}, cell impedance at start 11.2 mΩ and a reference power density p_{450} at 30 °C of 250 mW cm^{-2}.

way is to fit the almost straight current curve sections by straight lines as shown in Fig. 3. This fit is created by manual selection of five characteristic points, which describe the principle curve behaviour.

4.3. Statistical analysis of influence of operational parameters on $S_{q,max}$

A linear regression analyses was performed to predict the main influencing operational parameters on $S_{q,\max}$. Three parameters were found which have a significant impact on the value of $S_{q,\max}$. The largest effect has the reference power density p_{450}. The influence of the air flow rate u_{air} and the membrane humidity indicated by Z_{start} is lower. The coefficient correlation between these three parameters is lower than 0.4, this means that they are independent. Changes in the reference cell power density p_{450} are not due to potential changes of the membrane water uptake. During reference operation no significant changes of the cell impedance at 1000 Hz were observed.

Fig. 4 illustrates the regression result for $S_{q,\max}$ as predicted response graph. On the y-axis the predicted response from the

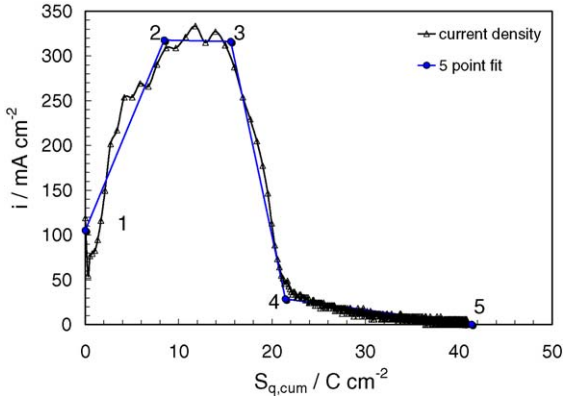

Fig. 3. Current density decay over cumulated charge transfer density $S_{q,\mathrm{cum}}(t)$ and manual fitted five-point curve. Cell voltage: 200 mV, cell temperature: −10 °C, gas flows: 600 ml_{air} min^{-1}, 120 ml_{H_2} min^{-1}, start impedance: 11.2 mΩ, reference power density: 250 mW cm^{-2}.

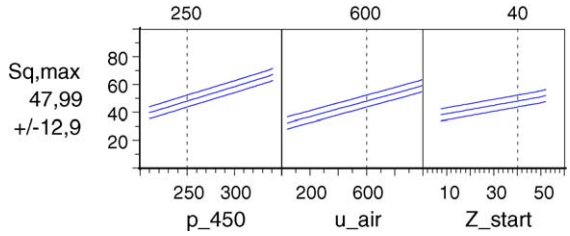

Fig. 4. Predicted $S_{q,\max}$ as function of the dominating three operational parameters. Linear regression of all operational parameters with a regression goodness of $R^2_{adj} = 0.87$ and a root mean squared error of 4.3 C cm^{-2}.

regression polynomial is shown as function of the values of p_{450} (250 mW cm^{-2}), u_{air} (600 ml min^{-1}) and Z_{start} (40 mΩ). The predicted value for $S_{q,\max}$ is 47.99 C cm^{-2} with a standard deviation of ±12.9 C cm^{-2}.

This result shows, that two operational factors can be adjusted by the operator to achieve a high load transfer rate. The membrane should be dry, indicated by a higher Z_{start} and the air flow rate should be also as high as possible. Both can be explained by the influence product water. The dryer the membrane, the higher is its water uptake and the higher the air flow, the better is the removal of product water on the cathode side. The third and most influencing parameter is p_{450}. This reference power density is strongly depending of the degradation status of the cathode electrode. When the electrode performance is low because of degradation, p_{450} is also lower. This means that during the potentiostatic cold start the output power and therefore the heat production is reduced too. This is why in the case of low p_{450} the electrode temperature is lower compared to cases with a higher p_{450}. This could lead to a faster flooding and ice formation in the electrodes.

4.4. Statistical analysis of the influence of components on $S_{q,max}$

The influence of components is strongly dominated by the GDL. The experiment space for the GDL porosity is too huge and therefore a statistical regression analysis is not able to show significantly the influence of the also investigated membrane thickness. $S_{q,\max}$ is mainly influenced by the GDL, p_{450} and the air flow u_{air}. The goodness of the regression analysis is not as high as for the operational parameters with $R^2_{adj} = 0.56$ and root mean squared error of 17.7 C cm^{-2}.

Fig. 5 illustrates the values of $S_{q,\max}$ grouped by the GDL configuration. A more open structure of the GDL leads to higher $S_{q,\max}$.

An interesting fact is that an open anode GDL structure led to the highest values for $S_{q,\max}$. This indicates that not only the cathode electrode is responsible for the inhibit of the reaction. Even at low temperatures a strong water permeation to the anode side seems to exist, otherwise the impact of the open anode channel structure could not be explained. Further investigations should be performed to find out, if primarily the cathode electrode freezes, as proposed by Kagami et al. [7], or if the anode electrode could also be affected by ice formation.

Table 3
Coefficients a_i for polynomial prediction model

	(1) I_{start} (mA cm^{-2})	(2) $S_{q,peak,start}$ (mA cm^{-2})	(2) I_{peak} (mA cm^{-2})	(3) $S_{q,peak,end}$ (mA cm^{-2})	(4) $S_{q,linear}$ (C cm^{-2})	(4) I_{linear} (mA cm^{-2})	(5) $S_{q,max}$ (mA cm^{-2})
Constant	−977.8981	−22.4874	144.9494	7.4862	3.9557	−1.9906	−26.0127
V	2.9383		−0.2209	−0.0180		−0.0056	
u_{air}	0.9819	0.0229	−0.4419	0.0104	−0.0024	0.0582	0.0247
u_{H_2}		0.6911		−0.6934			
Z_{start}	−36.3194	0.3027	−3.1301	0.3954	0.4184		0.4772
p_{450}	3.8487		0.1402			0.1094	0.1663
$u_{air}u_{H_2}$		−0.0008					
Vu_{air}	−0.0014					−0.0001	
VZ_{start}	0.0158		0.0036				
$p_{450}V$	−0.0104						
$u_{H_2}Z_{start}$		−0.0078		0.0107			
$u_{air}Z_{start}$	−0.0123	0.0004			0.0004		
$p_{450}u_{air}$			0.0021				
$p_{450}Z_{start}$	0.0888						
Uu_{H_2}				0.0009			

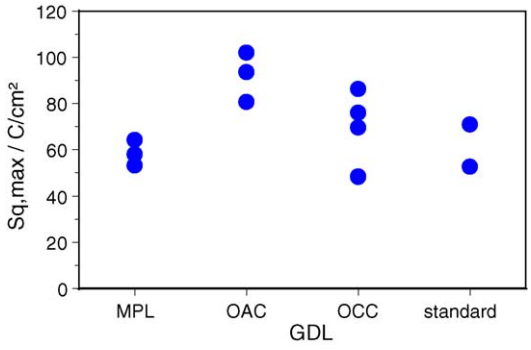

Fig. 5. $S_{q,max}$ as function of GDL configuration.

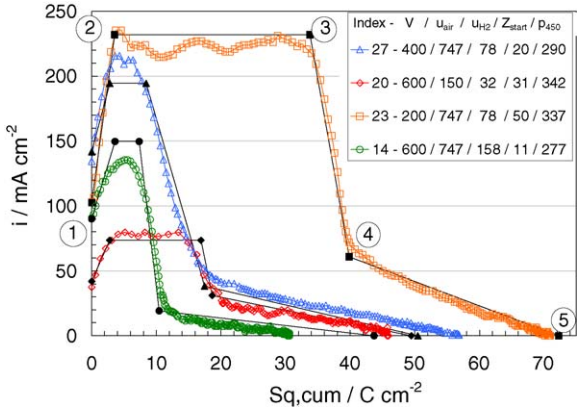

Fig. 6. Statistical based fit (filled symbols: ♦, ●, ■, ▲) of four current decay curves at −10 °C at different operating conditions as described in the legend.

4.5. *Influence of operational parameters on current decay and interpretation*

To find out which operational parameters affect the shape of the current decay curve linear regression analysis was made for each point (see Fig. 6). Interactions of the main parameters (U, u_{air}, u_{H_2}, Z_{start}, p_{450}) are included. The goodness of the regression analysis is indicated by R^2_{adj} which is for all points between 0.855 and 0.998, except for point 5 ($S_{q,max}$), where R^2_{adj} is 0.640. Table 3 shows all coefficients a_i for the statistic prediction polynomial.

As an example the regression model calculates $S_{q,linear}$ (point 4) with a polynomial expression, given by the constant c and factors a_i multiplied by the adjusted values influence parameter, in this example u_{air} and Z_{start}:

$$S_{q,linear} = 3.9557 - 0.0024u_{air} + 0.4184Z_{start} + 0.0004u_{air}Z_{start}$$

The quality of the model is demonstrated in Fig. 6. Points 1–4 are well fitted, point 5 not because of the low R^2_{adj}.

The statistic based model estimates the dominating factors for each curve point. In Table 4 the influence is shown.

The regression shows that the initial start current i_{start} is mainly depending on the membrane humidity Z_{start} and the

Table 4
Estimated influence of main parameters on current decay curves

Parameter	(1) i_{start} (%)	(2) $S_{q,peak,start}$ (%)	(2) i_{peak} (%)	(3) $S_{q,peak,end}$ (%)	(4) $S_{q,linear,start}$ (%)	(4) $i_{linear,start}$ (%)	(5) $S_{q,max}$ (%)
V	34	–	40	25	–	59	–
u_{air}	19	68	92	5	13	20	5
u_{H_2}	–	69	–	4	–	–	–
Z_{start}	43	36	32	87	85	–	26
p_{450}	12	–	34	–	–	10	26

operation voltage V. We assume that humidification of the membrane and the anode electrode sets in by product water until the current density reaches its peak plateau i_{peak}. The membrane reaches maximum protonic conductivity at $S_{q,peak,end}$. Now product water starts to fill mainly the pores of the electrodes and the current density drops down very fast. The level to which it drops down $i_{linear,start}$ is strongly dominated by the operating voltage V. Lower voltage is connected with higher waste heat production at the electrode resulting in a higher $i_{linear,start}$ because more product water stays in a liquid form and can be carried out by the air flow.

This interpretation is supported by the fact, that all charge transfer related statements are highly influenced by the drying status of the cell whereas all current related statements can be interpreted through heat production and are significantly influenced by the cell performance p_{450}, the cell voltage V and the air flow u_{air}.

These results show, that the presented current decay curves are very complex and depend on a variety of influence parameters. Existing physical fuel cell models cannot directly be applied. A combination of several model approaches is seen to be promising [7,8].

4.6. Performance loss by cold start experiments

In Fig. 7 the reference measurements at 450 mV before each cold start experiment is shown. A performance loss is obvious for each cell assembly. It is assumed that reduction of the effective catalyst surface could be made responsible for this decay. Oh et al. reported from catalyst layer degradation because of volume expansion during the phase change of liquid water to ice. The effective active surface is reduced and the pore size distribution in the catalyst layer changes [9]. Additionally slight changes of membrane properties could also affect the performance loss. McDonald et al. found out that membrane swelling by water uptake is reduced during freeze thaw cycling, but the electrochemical properties were not influenced [10].

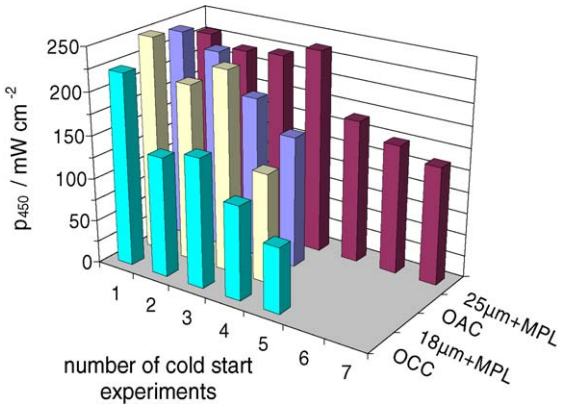

Fig. 7. Performance loss at 450 mV during four different cold start series. Reference measurements were performed at 30 °C cell temperature, dry reaction gases and constant stoichiometries of 1.5 for H_2 and 3.0 for air. The minimum measuring time for each data point was 20 min.

4.7. Conclusions of isothermal single cell experiments

Our statistical based model estimates the influencing parameters of isothermal cold start experiments of single fuel cells. The results support the work of Kagami et al., that a high air stream delays the reaction decay. Additionally the results show, that the influence of the starting impedance and the overall cell performance at 30 °C have an important influence too. We assume that a product water flux from the cathode to the anode influences the initial cold start behaviour in particular and also the time until the cell reaction is disrupted. It is found that the overall fuel cell performance at 450 mV and 30 °C is strongly affected by the cold start experiments and has also a strong influence on the cold start ability. The influence of the heat production connected with applied cell voltage for cold start is low at isothermal operation. Investigation of the component influence showed, that a high GDL porosity could enable a better water removal and therefore a higher cumulated charge transfer.

5. Results and discussion of fuel cell stack experiments

5.1. Cold start experiments at −10 °C

In a first test series the climate chamber was adjusted to a temperature of −10 °C. Three start up experiments were performed were the starting impedances were between 104 and 660 mΩ. The only regulation parameter was the applied load to the fuel cell stack.

Fig. 8 shows the first start up experiment at 1 A. In the graph the average single cell voltage of the stack with the minimum and maximum single cell voltages can be seen as well as stack temperature and stack current. The waste heat Q_{Waste} is also shown. It is calculated by (5) using the enthalpy of formation per mole $-\Delta\bar{h}_f$, the Faraday constant F, the average cell voltage V_{cell}, the number of cells n and the stack current I_{Stack}, assuming that the product water is condensed back to liquid [11]

$$Q_{Waste} = \left(\frac{-\Delta\bar{h}_f}{2F} - V_{cell}\right) n I_{Stack} \quad (5)$$

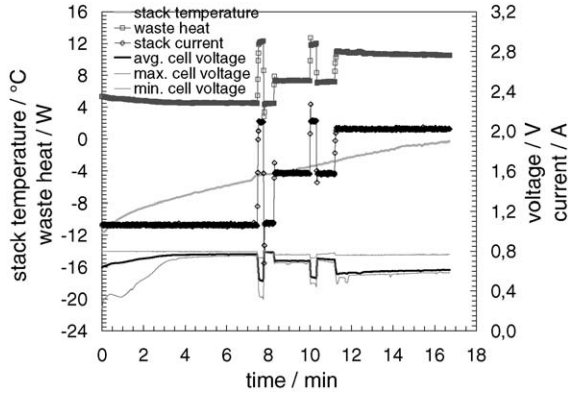

Fig. 8. Start up experiment of a six-cell fuel stack at −10 °C. The impedance at start was 660 mΩ, gas flow rates were 220 ml min^{-1} H_2 and 600 ml min^{-1} air.

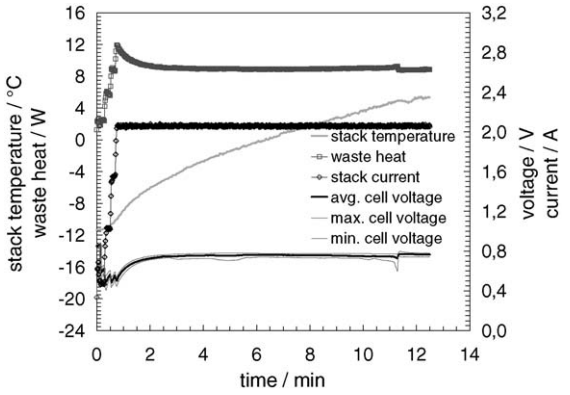

Fig. 9. Start up experiment of a six-cell fuel stack at −10 °C. The impedance at start was 230 mΩ, gas flow rates were 220 ml min^{-1} H_2 and 600 ml min^{-1} air.

In the beginning, the single cell voltages spread very strong between 260 and 800 mV. In the following the voltages converge. Responsible is the very dry state of the stack (Z_{start} = 660 mΩ) which is later humidified by product water. The stack temperature raised up to −5 °C within the first 7 min. Then the load was increased to 1.5 and 2 A. After 17 min the stack temperature reached 0 °C.

In Fig. 9 the start up is shown for a current increase to 2 A. The start impedance was 230 mΩ and therefore the single cell voltages are distributed more equally. The stack temperature increased in 6.5 min to 0 °C.

Fig. 10 illustrates an experiment with a current increase up to 2.8 A. The starting impedance was 100 mΩ. A temperature of 0 °C was reached within 4 min.

5.2. Cold start experiments at −20 °C

In a further test series the temperature was lowered to −20 °C. The gas flow rates were kept constant and the only start up regulation was done by adjustment of the applied load. Fig. 11 shows a cold start experiment at −20 °C. The cell reacts more sensitive, when load is applied than at −10 °C. It was not possible to reach 0 °C with passive methods whether in this case or other −20 °C cold start experiments.

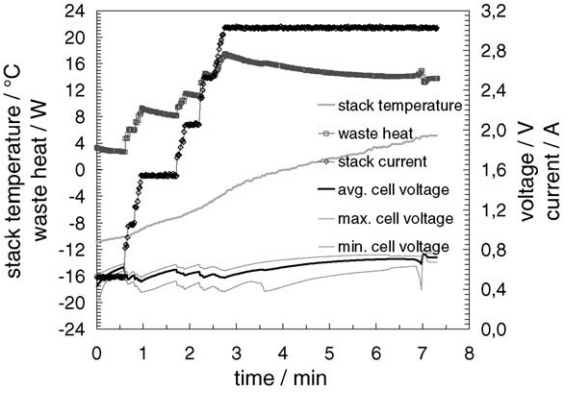

Fig. 10. Start up experiment of a six-cell fuel stack at −10 °C. The impedance at start was 100 mΩ, gas flow rates were 220 ml min^{-1} H_2 and 600 ml min^{-1} air.

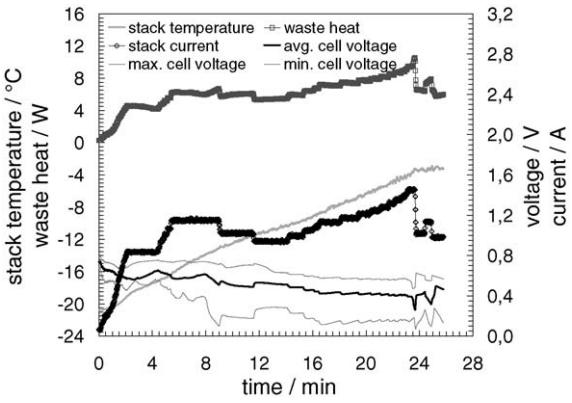

Fig. 11. Start up experiment of a six-cell fuel stack at −20 °C. The impedance at start was 120 mΩ, gas flow rates were 220 ml min^{-1} H_2 and 600 ml min^{-1} air.

5.3. Discussion of cold start experiments on portable fuel cell stacks

At temperatures of −10 °C and higher it was possible to start a portable fuel cell stack passive. In all experiments the stack temperature increased to operating temperatures over 40 °C at a constant ambient temperature of −10 °C. The impedance seems to have also in fuel cell stacks a strong influence on the start up behaviour. If the stack is too dry, the behaviour of the single cells differs strongly and does not allow an increase of load which would lead to a higher waste heat production of the stack. At −20 °C the single cells react very sensitive when load is applied. With the described experimental set-up a successful cold start up was not possible.

6. Conclusions

Substantial experiments of the cold start behaviour of fuel cells are presented, beginning with basic investigations on single cells and moreover cold start up experiments of portable fuel cell stacks in a climate chamber. An empirical based statistical model was introduced which describes the initial cold start behaviour of single cells in good correlation to experimental results. The main influencing operational parameters were identified. Results of the single cell experiments could be successfully adapted to start up portable stack from −10 °C. The load level must be high for a high waste heat level, the air flow rate should be high to blow out product water and for successful cold start up in fuel cell stacks the membrane should not be too dry. Degradation effects in single cells were observed resulting in lower performance at 30 °C.

References

[1] M. Cropper, Fuel cells for people, in: Proceedings of the Fuel Cell World, Luzern, 2003, pp. 43–54.
[2] C. Hebling, U. Groos, Brennstoffzellen im kleinen Leistungsbereich, f-cell, Documentation, Stuttgart, October 15, 2001.
[3] K. Tüber, M. Zobel, H. Schmidt, C. Hebling, A polymer electrolyte membrane fuel cell system for powering portable computers, J. Power Sources 122 (2003) 1–8.

[4] A. Kabza, J. Kaczerowski, M. Götz, M. Neugebauer, H. Locher, J. Scholta, L. Jörissen, J. Garche, Development of low pressure self humidifying PEFC stacks and systems, in: Proceedings of the Second European PEFC Forum, vol. 1, 2003, pp. 801–811.
[5] T. Wember, Instruction Material for Cornerstone Training Course, Technische Statistik und statistische Versuchsplanung, 2001.
[6] A. Handl, Skript zur Grundausbildung in Statistik mit R, Fakultät für Wirtschaftswissenschaften, Universität Bielefeld, 2003. http://www.wiwi.uni-bielefeld.de/~frohn/Lehre/Statistik1/Skript/stat12b.pdf.
[7] F. Kagami, Y. Hishinuma, T. Chikahisa, Performance and self-starting of a PEFC at temperatures below freezing, Therm. Sci. Eng. 10 (3) (2002) 25–33.
[8] G. Maggio, V. Recupero, L. Pino, Modelling polymerelectrolyte fuel cells: an innovative approach, J. Power Sources 101 (2001) 275–286.
[9] I.-H. Oh, E. Cho, H.Y. Ha, S.-A. Hong, Effect of water freezing on the performance of PEMFC, in: Proceedings of the Second European PEFC Forum, vol. 1, 2003, pp. 413–418.
[10] R.C. McDonald, C.K. Mittelsteadt, E.L. Thompson, Freeze–thaw cycling of proton-exchange membranes: electrochemical and mechanical analyses, in: Proceedings of the Second European PEFC Forum, vol. 1, 2003, pp. 199–207.
[11] J. Larminie, A. Dicks, Fuel Cell Systems Explained, 1st ed., Wiley, Chichester, 1999.